Research Square

Preprints are preliminary reports that have not undergone peer review.
They should not be considered conclusive, used to inform clinical practice,
or referenced by the media as validated information.

T2-weighted MRI-based radiomics for preoperative prediction of homologous recombination deficiency status in high-grade serous ovarian carcinoma

Jianan Zhou
Women's Hospital, School of Medicine, Zhejiang University
Xinang Jiang
Third Affiliated Hospital of Naval Medical University
Meixiang Deng
Women's Hospital, School of Medicine, Zhejiang University
Kui Li
Women's Hospital, School of Medicine, Zhejiang University
Yuanming Shen
Women's Hospital, School of Medicine, Zhejiang University
Yu Zou
zouyuzju@zju.edu.cn

Women's Hospital, School of Medicine, Zhejiang University

Research Article

Keywords: Radiomics, Magnetic Resonance Imaging, Homologous Recombination Deficiency, High-grade Serous Ovarian Carcinoma

Posted Date: June 22nd, 2026

DOI: https://doi.org/10.21203/rs.3.rs-10018099/v1

License: This work is licensed under a Creative Commons Attribution 4.0 International License.
Read Full License

Additional Declarations: No competing interests reported.

Abstract

Rationale and objectives:

The aim of this study was to explore the feasibility of T2-weighted imaging (T2WI) - based radiomics in preoperative prediction of homologous recombination deficiency (HRD) status in patients with high-grade serous ovarian carcinoma (HGSOC), and to establish a non-invasive approach for guiding individualized treatment planning.

Materials and methods

A total of 133 patients with pathologically confirmed HGSOC who underwent MRI scan (T2WI) were retrospectively enrolled in this study. All patients were stratified into HRD-positive and HRD-negative group. These 133 patients (41 in HRD-negative group and 92 in HRD-positive group) were randomly allocated to a training set (n = 93) and a validation set (n = 40) at a 7:3 ratio. Three different models were constructed and evaluated: clinical characteristics only (clinical model); T2WI-radiomics features only (radiomics model); and a combination of them all (combined model). The predictive performance was evaluated using the receiver operating characteristic (ROC) analysis, and area under the curves (AUCs) were compared using the DeLong test. Calibration curves and decision curve analysis (DCA) were applied to validate the clinical-radiomic combined model.

Results

In the training set, the combined model achieved the best performance (AUC = 0.889; all P > 0.05). The radiomics model achieved predictive performance comparable to the clinical model (AUC of 0.762 vs. 0.790; P = 0.676). In the validation set, the combined model performed significantly better than the clinical or radiomics model (AUCs of 0.853 vs. 0.805 vs. 0.706; all P > 0.05). DCA demonstrated that the combined model achieved superior net benefit across a wide range of threshold probabilities compared with the clinical and radiomics models alone.

Conclusions

Our research demonstrated that the combined model achieved the optimal predictive performance. It is feasible to apply radiomics to predict HRD status of HGSOC patients, which can further assist clinicians in formulating individualized treatment strategies.

1. Introduction

Ovarian cancer has the highest mortality rate among gynecologic malignancies, with high-grade serous ovarian carcinoma (HGSOC) being the most common histological subtype, accounting for approximately

70%–80% of all cases(1). Although a majority of patients with HGSOC exhibit initial sensitivity to platinum-based chemotherapy, tumor recurrence and chemoresistance remain major clinical challenges(2). In recent years, the introduction of poly ADP-ribose polymerase inhibitors (PARPi) has provided new therapeutic opportunities for HGSOC patients(3). The efficacy of PARPi is primarily dependent on the presence of homologous recombination deficiency (HRD) within the tumor cells.

HRD status has emerged as a crucial biomarker for guiding precision therapy in HGSOC patients, closely correlating with sensitivity to platinum-based chemotherapy and the efficacy of PARPi. However, its widespread clinical implementation faces numerous challenges(4–6). First, the high cost of HRD testing platforms limits their broad applicability, as they are not yet reimbursed by national health insurance systems in many countries and regions(7). Second, a lack of standardization across different platforms, which employ varying algorithms and thresholds for genomic instability scoring, poses issues regarding the comparability and reproducibility of results(8, 9). Furthermore, tumor heterogeneity and clonal evolution may compromise the accurate assessment of HRD status, particularly in the recurrent or metastatic setting. More notably, approximately 60%-70% of patients with HRD-positive tumors are actually breast cancer susceptibility gene (BRCA) wild-type, with HRD arising from other mechanisms such as mutations in other homologous recombination repair genes or BRCA promoter methylation(10). This suggests that reliance on BRCA testing alone would miss a substantial number of patients who could potentially benefit from PARPi(11). Therefore, achieving accurate, accessible, and cost-effective assessment of HRD status represents a critical issue demanding urgent resolution in the era of precision oncology for ovarian cancer.

Studies have demonstrated that HRD-positive patients exhibit higher sensitivity to platinum-based chemotherapy and derive significant progression-free survival benefits from PARPi maintenance therapy. In the PRIMA trial, patients with HRD-positive tumors who received niraparib maintenance therapy achieved a significantly longer median progression-free survival compared to the placebo group (21.9 months vs. 10.4 months), with substantial benefit also observed in the HRD-positive subgroup without BRCA mutations (22.1 months vs. 10.9 months)(12). The PAOLA-1 trial further confirmed that maintenance therapy with olaparib in combination with bevacizumab significantly reduced the risk of death in HRD-positive patients(13). Based on this body of evidence, both the National Comprehensive Cancer Network and the European Society for Medical Oncology guidelines strongly recommend HRD testing in patients with HGSOC to identify those most likely to benefit from PARPi therapy.

Radiomics, as an emerging non-invasive analytical approach, enables the high-throughput extraction of quantitative features from images, thereby comprehensively reflecting the overall heterogeneity and biological behavior of tumors. Compared with traditional tissue biopsy, radiomics offers advantages such as non-invasiveness, reproducibility, and the ability to overcome tumor heterogeneity(14). A recent study(15) based on CT radiomics preliminarily demonstrated that combining intra- and peritumoral imaging features can effectively predict HRD scores and HRD status in ovarian cancer patients, achieving an area under the curve (AUC) of 0.85–0.87 in the training cohort. This provides a novel approach for non-invasive assessment of HRD status. However, research on radiomics-based prediction of HRD status is still in early stages and has several limitations. Firstly, most existing studies have utilized CT imaging(16),

whereas MRI offers superior soft tissue resolution and unique advantages in evaluating ovarian tumors. Secondly, T2-weighted imaging (T2WI), as a routine MRI sequence, is widely available and well-standardized in clinical practice; however, whether T2WI-based radiomics can effectively predict HRD status remains systematically unexplored.

This study aims to investigate the value of a T2WI-based radiomics model for predicting HRD status in HGOSC. By integrating radiomic features with clinicopathological characteristics, we seek to develop a comprehensive predictive model. This approach is intended to provide a cost-effective, accessible, and non-invasive tool for screening HRD status in HGSOC patients, thereby optimizing the selection strategy for patients likely to benefit from PARPi therapy and advancing the clinical practice of precision medicine in ovarian cancer.

2. Materials and methods

2.1. Patient selection and clinical data

This retrospective study was approved by the Institutional Review Board of ***, which waived the requirement for informed consent. A total of 261 patients with surgically and pathologically confirmed HGSOC between January 2024 and December 2025 were retrospectively identified. The inclusion criteria were as follows: (1) female, aged ≥ 18 years; (2) pathologically confirmed HGSOC; (3) underwent preoperative pelvic MRI scan (T2WI) within 4 weeks prior to surgery; (4) complete clinical data available (including age, carbohydrate antigen 125 (CA125), carcinoembryonic antigen (CEA), human epididymis protein 4 (HE4), and menopausal status, et al); and (5) genetic testing results (BRCA1/2 mutation status and HRD status). The exclusion criteria were as follows: (1) prior radiotherapy, chemotherapy, or targeted therapy before surgery; (2) recurrent HGSOC or a history of other malignancies; (3) poor image quality precluding satisfactory analysis; (4) incomplete clinical or pathological data; and (5) pregnancy or lactation. The details of the recruitment process were shown in Fig. 1.

All enrolled patients were stratified into two groups according to the status of HRD: HRD-positive group and HRD-negative group. The HRD status was assessed by next-generation sequencing of tumor tissue using the kit provided by the Myriad Genetics myChoice® HRD assay platform(10). Finally, 133 eligible patients (41 in HRD-negative group and 92 in HRD-positive group) were randomly divided into a training set and a validation set at a ratio of 7:3 using a random number table, resulting in 93 patients in the training set and 40 patients in the validation set.

2.2. Image acquisition and tumor segmentation

Pelvic MRI was performed using a GE Signa HDxt 1.5T MR scanner equipped with a 16-channel cardiac coil. The scanning range extended from the lower margin of the pubic symphysis to the line connecting the anterior superior iliac spines. Axial T2WI were acquired with the following standardized parameters: repetition time = 3,100 ms, echo time = 73 ms, field of view = 280 mm × 280 mm, slice thickness = 4–6 mm, and intersection gap = 1 mm.

Tumor volumes of interests (VOIs) containing both cystic and solid components were manually delineated slice by slice on T2WI using ITK-SNAP software (v.3.8.0, http://www.itksnap.org). Two independent researchers (with 5 and 10 years of experience in abdominal imaging, respectively) reviewed the clinical data and MRI images to ensure accuracy. Radiologist A, with 10 years of experience in pelvic MRI diagnosis, initially segmented the VOIs for all subjects. To evaluate interobserver reproducibility, the VOIs of 30 randomly selected patients from the training set were segmented by another radiologist (Radiologist B) who had 5 years of experience in pelvic MRI diagnosis. For the assessment of intraobserver reproducibility, Radiologist A repeated the segmentation procedure for all patients after a one-month interval. The interobserver and intraobserver reproducibility of VOI segmentation was evaluated using intraclass correlation coefficients (ICCs), with ICCs > 0.80 considered to have good stability and reproducibility. The initial segmentation results obtained by Radiologist A were used for model construction.

Referring to previous studies(17, 18), the two radiologists who performed VOI delineation also independently assessed the following conventional MRI features: (1) tumor location; (2) tumor shape; (3) texture, classified as cystic-solid and solid; (4) hemorrhage; (5) enhancement intensity compared to myometrium; and (6) ascites. Any discrepancies between the two radiologists were resolved through consensus review. Both radiologists were kept blinded to the histopathological results and clinical information of the tumors during image review.

2.3. Feature extraction and selection

Before feature extraction, the image underwent a three-step preprocessing procedure. These steps included voxel resampling, gray discretization, and image intensity normalization. Subsequently, Radiomics features were extracted using the open-source software pyradiomics (version 3.0.1, https://pyradiomics.readthedocs.io/en/latest/). Three types of features were obtained: first-order features, shape features, and texture features. Radiomics features of the entire tumor, which exhibited considerable data dispersion, were processed by z-score standardization. Finally, a total of 1197 radiomics features were extracted. Two feature selection methods, maximum relevance minimum redundancy and least absolute shrinkage and selection operator (LASSO), were used to select the feature. Before LASSO regression, maximum relevance minimum redundancy was performed to eliminate the redundant and irrelevant features. Then LASSO was conducted to choose the optimized subset of features to construct the final model. LASSO analysis included choosing the regular parameter λ, determining the number of the feature. Finally, the radiomics signature was constructed by using 7 features (Fig. 1). The Radscore was calculated using the following formula: Radscore = 0.6559139784946252 + 0.002604 * log_sigma_2_0_mm_3D_firstorder_90Percentile_T2WI + 0.026943 * log_sigma_4_0_mm_3D_firstorder_Kurtosis_T2WI -0.052810 * log_sigma_4_0_mm_3D_gldm_LargeDependenceLowGrayLevelEmphasis_T2WI + 0.032930 * log_sigma_5_0_mm_3D_firstorder_90Percentile_T2WI -0.010340 * log_sigma_5_0_mm_3D_firstorder_Skewness_T2WI -0.025767 * log_sigma_5_0_mm_3D_gldm_LargeDependenceLowGrayLevelEmphasis_T2WI -0.037854 *

original_shape_Flatness_T2WI -0.032192 * wavelet_HLH_firstorder_RootMeanSquared_T2WI + 0.008200 * wavelet_HLL_firstorder_Mean_T2WI + 0.007742 * wavelet_LLH_firstorder_RootMeanSquared_T2WI.

2.4. Models building and evaluation

Clinical variables with significant differences between HRD-negative group and HRD-positive group were incorporated to construct a clinical model. Based on the selected radiomics features, a radiomics signature was constructed by calculating the radiomics score (Rad-score) for each patient using a linear combination of the selected features weighted by their respective coefficients from the LASSO regression.

A clinical-radiomic combined model was further established by integrating the Rad-score and the independent clinical predictive factors. The predictive performance of the three models (clinical model, radiomics model, and combined model) was evaluated using the AUC in both the training set and the validation set.

Calibration curves were plotted to assess the consistency between the predicted probability of HRD status and the actual HRD status, and the Hosmer-Lemeshow (H-L) test was used to test the calibration effect ($P > 0.05$ indicated good calibration). Decision curve analysis (DCA) was performed to evaluate the clinical utility of the models by calculating the net benefit at different threshold probabilities, a higher net benefit indicated better clinical value of the model.

2.5. Statistical analysis

Measurements were analyzed using SPSS 25.0 (IBM) and R 4.3.1 (https://www.R-project.org). Continuous variables were presented as mean ± standard deviation (SD), and categorical variables as proportions. Normality of quantitative variables was assessed by the Shapiro–Wilk test. Normally distributed data were compared using the independent-sample t test, and non-normally distributed data using the Mann–Whitney U test. Categorical variables were analyzed with the chi-square test or Fisher exact test, as appropriate. $P < 0.05$ was considered statistically significant. Receiver operating characteristic (ROC) curves were constructed to evaluate the model's predictive performance. The DeLong test was used to assess whether differences in model performance were statistically significant.

3. Results

3.1. Data set

A total of 133 patients (41 in HRD-negative group and 92 in HRD-positive group) were recruited in this study. The training set included 93 patients (32 HRD-negative [age 58.84 ± 10.79 years] and 61 HRD-positive [age 57.66 ± 9.73]). The validation set included 40 patients (9 HRD-negative [age 53.89 ± 11.23] and 31 HRD-positive [age 55.58 ± 7.32]).

In the training set and validation set, significant differences were identified for BRCA mutation status (all $P < 0.05$). Comparing the HRD-negative and HRD-positive groups, progesterone receptor (PR) status was significantly different ($P < 0.05$) in the training set and tumor shape was significantly different ($P = 0.024$)

in the validation set. There were no significant differences observed in terms of six clinical characteristics (age, CA125, CEA, HE4, menopausal status, and Federation of International of Gynecologists and Obstetricians (FIGO) stage), five radiological characteristics (tumor location, characteristics, hemorrhage, enhancement intensity, and ascites), and three pathological characteristics (Ki-67 level, estrogen receptor (ER) status, and P53 status) (all $P > 0.05$) between the two datasets. The detailed information on the clinical and radiological characteristics of the enrolled patients was summarized in Table 1.

Table 1
Clinical and radiological characteristics of HGSOC patients in training set and validation set

Variables	training set (n = 93)		*P*	validation set (n = 40)		*P*
	HRD-negative (n = 32)	HRD-positive (n = 61)		HRD-negative (n = 9)	HRD-positive (n = 31)	
Age, Mean ± SD	58.84 ± 10.79	57.66 ± 9.73	0.591	53.89 ± 11.23	55.58 ± 7.32	0.593
CA125, Mean ± SD	1400.36 ± 3964.58	1646.43 ± 8675.92	0.879	732.98 ± 1123.77	1331.11 ± 1652.85	0.317
CEA, Mean ± SD	1.83 ± 2.10	2.58 ± 5.40	0.486	9.66 ± 19.35	1.38 ± 1.04	0.301
HE4, Mean ± SD	556.49 ± 1092.31	420.11 ± 436.60	0.400	199.52 ± 241.70	431.01 ± 367.64	0.087
Menopausal status, n (%)			0.924			0.642
Premenopausal	5 (15.62)	10 (16.39)		4 (44.44)	9 (29.03)	
Postmenopausal	27 (84.38)	51 (83.61)		5 (55.56)	22 (70.97)	
Location, n (%)			0.335			0.097
Unilateral	17 (53.12)	26 (42.62)		6 (66.67)	9 (29.03)	
Bilateral	15 (46.88)	35 (57.38)		3 (33.33)	22 (70.97)	
Shape, n (%)			0.777			**0.024**
Irregular	14 (43.75)	26 (42.62)		1 (11.11)	16 (51.61)	
Lobulated	4 (12.50)	11 (18.03)		3 (33.33)	10 (32.26)	
Oval	14 (43.75)	24 (39.34)		5 (55.56)	5 (16.13)	
Characteristics, n (%)			0.345			0.367
Cystic-solid	26 (81.25)	45 (73.77)		9 (100.00)	25 (80.65)	
Solid	6 (18.75)	16 (26.23)		0 (0.00)	6 (19.35)	
Hemorrhage, n (%)			0.940			0.557
None	29 (90.62)	57 (93.44)		9 (100.00)	27 (87.10)	

Abbreviations: HGSOC, high-grade serous ovarian carcinoma; HRD, homologous recombination deficiency; SD, standard deviation; CA125, carbohydrate antigen 125; CEA, carcinoembryonic antigen; HE4, human epididymis protein 4; Ki-67, proliferation marker protein; BRCA, breast cancer susceptibility gene; ER, estrogen receptor; PR, progesterone receptor; FIGO, Federation of International of Gynecologists and Obstetricians.

Variables	training set (n = 93)		*P*	validation set (n = 40)		*P*
	HRD-negative (n = 32)	HRD-positive (n = 61)		HRD-negative (n = 9)	HRD-positive (n = 31)	
Yes	3 (9.38)	4 (6.56)		0 (0.00)	4 (12.90)	
Enhancement intensity, n (%)			0.405			1.000
Hyperintense	16 (50.00)	36 (59.02)		6 (66.67)	22 (70.97)	
Hypointense	16 (50.00)	25 (40.98)		3 (33.33)	9 (29.03)	
Ascites, n (%)			0.645			0.668
None	9 (28.12)	20 (32.79)		2 (22.22)	3 (9.68)	
Yes	23 (71.88)	41 (67.21)		7 (77.78)	28 (90.32)	
Ki-67, n (%)			1.000			1.000
≤ 20%	2 (6.25)	3 (4.92)		0 (0.00)	2 (6.45)	
>20%	30 (93.75)	58 (95.08)		9 (100.00)	29 (93.55)	
BRCA, n (%)			**< .001**			**0.035**
Mutated	3 (9.38)	28 (45.90)		0 (0.00)	14 (45.16)	
Wild-type	29 (90.62)	33 (54.10)		9 (100.00)	17 (54.84)	
ER, n (%)			0.300			0.545
Negative	5 (15.62)	4 (6.56)		1 (11.11)	2 (6.45)	
Positive	27 (84.38)	57 (93.44)		8 (88.89)	29 (93.55)	
PR, n (%)			**< .001**			0.190
Negative	29 (90.62)	31 (50.82)		8 (88.89)	18 (58.06)	
Positive	3 (9.38)	30 (49.18)		1 (11.11)	13 (41.94)	
P53, n (%)			0.227			0.121
Mutated	29 (90.62)	60 (98.36)		7 (77.78)	30 (96.77)	
Wild-type	3 (9.38)	1 (1.64)		2 (22.22)	1 (3.23)	
FIGO, n (%)			0.121			1.000

Abbreviations: HGSOC, high-grade serous ovarian carcinoma; HRD, homologous recombination deficiency; SD, standard deviation; CA125, carbohydrate antigen 125; CEA, carcinoembryonic antigen; HE4, human epididymis protein 4; Ki-67, proliferation marker protein; BRCA, breast cancer susceptibility gene; ER, estrogen receptor; PR, progesterone receptor; FIGO, Federation of International of Gynecologists and Obstetricians.

Variables	training set (n = 93)		*P*	validation set (n = 40)		*P*
	HRD-negative (n = 32)	HRD-positive (n = 61)		HRD-negative (n = 9)	HRD-positive (n = 31)	
□+□	9 (28.12)	9 (14.75)		2 (22.22)	6 (19.35)	
□+□	23 (71.88)	52 (85.25)		7 (77.78)	25 (80.65)	

Abbreviations: HGSOC, high-grade serous ovarian carcinoma; HRD, homologous recombination deficiency; SD, standard deviation; CA125, carbohydrate antigen 125; CEA, carcinoembryonic antigen; HE4, human epididymis protein 4; Ki-67, proliferation marker protein; BRCA, breast cancer susceptibility gene; ER, estrogen receptor; PR, progesterone receptor; FIGO, Federation of International of Gynecologists and Obstetricians.

3.2. Univariate and multivariate logistic regression analysis of factors associated with HRD status

Univariate logistic regression analysis was performed to identify clinical, radiological, and pathological factors associated with HRD status. As shown in Table 2, BRCA mutation (Odds Ratio (OR) = 0.12, 95% Confidence Interval (CI): 0.03–0.44, P = 0.001) and PR positivity (OR = 9.35, 95% CI: 2.57–33.99, P < 0.001) were significantly associated with HRD status. No other variables, including age, CA125, CEA, HE4, menopausal status, tumor location, characteristics, shape, hemorrhage, enhancement intensity, ascites, Ki-67, ER, P53, or FIGO stage, reached statistical significance (all P > 0.05).

Table 2
Results of univariate and multivariate logistic regression

Variables	univariate logistic regression				multivariate logistic regression			
	β	Z	*P*	OR (95%CI)	β	Z	*P*	OR (95%CI)
Age	-0.01	-0.54	0.587	0.99 (0.95 ~ 1.03)				
CA125	0.00	0.15	0.878	1.00 (1.00 ~ 1.00)				
CEA	0.06	0.64	0.525	1.06 (0.89 ~ 1.26)				
HE4	-0.00	-0.81	0.416	1.00 (1.00 ~ 1.00)				
Menopausal status	-0.06	-0.10	0.924	0.94 (0.29 ~ 3.04)				
Location	0.42	0.96	0.336	1.53 (0.65 ~ 3.61)				
Characteristics	16.55	0.01	0.991	15354167.60 (0.00 ~ Inf)				
Shape	-0.08	-0.17	0.865	0.92 (0.37 ~ 2.33)				
Hemorrhage	-0.39	-0.49	0.626	0.68 (0.14 ~ 3.24)				
Enhancement intensity	-0.36	-0.83	0.406	0.69 (0.29 ~ 1.64)				
Ascites	-0.22	-0.46	0.645	0.80 (0.31 ~ 2.05)				
Ki-67	0.25	0.27	0.787	1.29 (0.20 ~ 8.14)				
BRCA	-2.10	-3.20	**0.001**	0.12 (0.03 ~ 0.44)	-2.11	-3.07	**0.002**	0.12 (0.03 ~ 0.47)
ER	0.97	1.37	0.172	2.64 (0.66 ~ 10.62)				
PR	2.24	3.40	**< .001**	9.35 (2.57 ~ 33.99)	2.24	3.28	**0.001**	9.40 (2.46 ~ 35.86)

Abbreviations: OR, odds ratio; CI, confidence interval; CA125, carbohydrate antigen 125; CEA, carcinoembryonic antigen; HE4, human epididymis protein 4; Ki-67, proliferation marker protein; BRCA, breast cancer susceptibility gene; ER, estrogen receptor; PR, progesterone receptor; FIGO, Federation of International of Gynecologists and Obstetricians

Variables	univariate logistic regression				multivariate logistic regression			
	β	Z	*P*	OR (95%CI)	β	Z	*P*	OR (95%CI)
P53	-1.83	-1.55	0.121	0.16 (0.02 ~ 1.62)				
FIGO	0.82	1.53	0.126	2.26 (0.79 ~ 6.44)				

Abbreviations: OR, odds ratio; CI, confidence interval; CA125, carbohydrate antigen 125; CEA, carcinoembryonic antigen; HE4, human epididymis protein 4; Ki-67, proliferation marker protein; BRCA, breast cancer susceptibility gene; ER, estrogen receptor; PR, progesterone receptor; FIGO, Federation of International of Gynecologists and Obstetricians

Multivariate logistic regression analysis was subsequently conducted incorporating variables with $P < 0.05$ in the univariate analysis. The results demonstrated that PR positivity remained an independent predictor of HRD positivity (OR = 9.40, 95% CI: 2.46–35.86, P = 0.001). Similarly, BRCA mutation maintained its significant inverse association with HRD negativity (OR = 0.12, 95% CI: 0.03–0.47, P = 0.002), indicating that BRCA-mutated tumors were more likely to be HRD-positive (Table 2).

3.3. Models building and evaluation

The diagnostic performance of the clinical model, radiomics model, and combined model for predicting HRD status was evaluated in both the training and validation cohorts (Table 3).

Table 3
Diagnostic performances of different models

Cohort	Models	AUC	95% CI	Accuracy	Sensitivity	Specificity	PPV	NPV
Training set	Clinical	0.790	0.707–0.873	0.753	0.721	0.813	0.880	0.605
	Radiomics	0.762	0.663–0.861	0.656	0.525	0.906	0.914	0.500
	Combined	0.889	0.821–0.958	0.817	0.771	0.906	0.940	0.674
Validation set	Clinical	0.805	0.654–0.956	0.775	0.742	0.889	0.958	0.500
	Radiomics	0.706	0.523–0.889	0.650	0.613	0.778	0.905	0.368
	Combined	0.853	0.688–1.000	0.875	0.871	0.889	0.964	0.667

Abbreviations: AUC, area under the curve; CI, confidence interval; PPV, positive predictive value; NPV, negative predictive value

In the training set, the combined model achieved the highest AUC of 0.889 (95% CI: 0.821–0.958), outperforming the clinical model (AUC = 0.790, 95% CI: 0.707–0.873) and the radiomics model (AUC = 0.762, 95% CI: 0.663–0.861). The combined model also demonstrated superior accuracy (0.817), sensitivity (0.771), specificity (0.906), positive predictive value (PPV) (0.940), and negative predictive value (NPV) (0.674) compared with the other two models.

In the validation set, consistent results were observed. The combined model yielded the highest AUC of 0.853 (95% CI: 0.688–1.000), followed by the clinical model (AUC = 0.805, 95% CI: 0.654–0.956) and the radiomics model (AUC = 0.706, 95% CI: 0.523–0.889). Notably, the combined model achieved the best accuracy (0.875), sensitivity (0.871), specificity (0.889), PPV (0.964), and NPV (0.667) in the validation set, indicating robust generalizability. The ROC curves for the three models in the training set and validation set were presented in Fig. 2(A) and Fig. 2(B). The two independent predictors (including BRCA mutation and PR status) were incorporated into the nomogram (Fig. 2(C)).

3.4. Model differences and clinical utility of models

There were no significant differences in AUCs between the clinical and radiomics models in the training and validation set (P > 0.05 [Delong test]). In the training set, the AUC values of the combined model were significantly better than that of the clinical model (P = 0.003 [Delong test]) or radiomics model (P = 0.002 [Delong test]) (Supplementary Table 1).Although the AUC of the combined model showed no significant differences compared with the clinical model and radiomics model in the validation set (all P > 0.05 [Delong test]), the combined model yielded significantly higher accuracy, sensitivity and specificity than the other two models.

Through the H-L test, calibration curves indicated that there was no significant departure between prediction and observation in the training and validation set (Fig. 3(A)). In the validation set, the H-L test yielded P values of 1.000, 0.323, and 0.184 for the clinical, radiomics, and combined models, respectively, indicating good calibration for all models (all P > 0.05). The DCA, which balanced the benefits of the model against its costs, was used to calculate the net benefit of the model at various cutoff values to evaluate its performance. As shown in Fig. 3(B), both predictive models in this study provided better predictive performance compared to the “no model” approach across all thresholds. Besides, the combined model outperformed the clinical model and radiomics model at most thresholds.

4. Discussion

In this study, we developed and validated a T2WI-based clinical-radiomics combined model for the preoperative prediction of HRD status in patients with HGSOC. The combined model demonstrated excellent discriminatory performance in both the training set and the validation set, significantly outperforming the clinical model and the radiomics model. Collectively, these findings indicate that the combined model serves as a robust, non-invasive, and clinically applicable tool for preoperatively predicting HRD status in HGSOC patients, thereby potentially facilitating personalized treatment decisions.

To date, several radiomics-based studies have attempted to predict HRD status or BRCA mutations in ovarian cancer, most of which have been predominantly based on CT images(19, 20). For instance, Wu et al. developed a CT-based radiomics signature for predicting HRD score and status based on intra- and peritumoral radiomics with AUCs of 0.852 and 0.781 in the training and validation cohort for predicting HRD score, respectively; with AUCs of 0.874 and 0.824 in the training and validation cohort for predicting HRD status, respectively(15). Similarly, other investigators have explored CT-derived features to distinguish BRCA mutated from BRCA wild-type tumors, with moderate predictive performance(21). In comparison, the present study specifically focused on T2WI(22), which possesses several inherent advantages over CT for characterizing ovarian tumors. Firstly, T2WI provides superior soft tissue contrast, enabling more precise delineation of tumor morphology, including cystic-solid components, hemorrhage, necrosis, and septations, all of which may reflect underlying genomic instability. Secondly, T2WI is acquired without ionizing radiation, making it a safer alternative for patients of reproductive age who may require serial imaging for treatment monitoring. Thirdly, the superior resolution of T2WI allows for more accurate segmentation and feature extraction, potentially capturing subtle textural alterations that correlate with HRD status. To the best of our knowledge, the application of T2WI-based radiomics specifically for HRD prediction in HGSOC remains underexplored. Our proposed combined model achieved an AUC of 0.889 in the training set and 0.853 in the validation set, which is comparable to or even exceeds the performance of previously reported CT-based models. Notably, our clinical-radiomics integrated strategy consistently outperformed the standalone radiomics model, a finding that aligns with emerging evidence suggesting that complementary information from clinical variables (particularly PR and BRCA status) and imaging features can synergistically enhance predictive accuracy.

The identification of PR positivity and BRCA mutation status as independent predictors of HRD positivity in our study warrants further biological interpretation. Although ER and PR are traditionally considered prognostic markers in ovarian cancer, their relationship with homologous recombination repair deficiency has not been extensively characterized. One plausible explanation is that PR-positive tumors may exhibit an enhanced dependency on DNA repair pathways, and the loss of PR signaling could lead to genomic instability. Alternatively, PR expression might serve as a surrogate marker for a specific molecular subtype of HGSOC that is inherently more susceptible to DNA damage and repair dysfunction(23). As expected, BRCA mutation emerged as another strong independent predictor of HRD positivity, align with the well-established biological paradigm that germline or somatic mutations in BRCA1/2 genes disrupt the homologous recombination repair machinery, leading to genomic instability and the characteristic "BRCAness" phenotype(24, 25). Our results indicated a strong correlation between BRCA mutation status and HRD positivity, which was highly consistent with previous reports(26). Studies have shown that up to 50% of patients with HGSOC exhibit HRD through mechanisms such as germline or somatic BRCA mutations and BRCA promoter methylation. This phenomenon is closely associated with the molecular characteristics and genomic instability inherent to HGSOC(27, 28). These mechanisms impair homologous recombination (HR) repair, which not only contributes to tumorigenesis but also concurrently increases tumor sensitivity to platinum-based chemotherapy(29).

Regarding imaging features, although not retained in the multivariate model, several radiological characteristics demonstrated notable associations with HRD status in the descriptive analysis. Several previous studies have reported the MRI features as a predictor of ovarian cancer(30–32). In our study, HRD-positive tumors exhibited a higher prevalence of bilateral involvement and irregular shape compared with their HRD-negative counterparts. These morphological features are consistent with the aggressive biological behavior and high-grade nature of HRD-positive HGSOC, which often presents with rapid growth and significant intratumoral heterogeneity(33). The irregular shape, in particular, may reflect infiltrative growth patterns and desmoplastic stromal reactions, both of which are hallmarks of genomically unstable tumors. Notably, the validation set demonstrated a statistically significant difference in shape distribution, further supporting the discriminative potential of morphological features. The cystic-solid composition and enhancement intensity, however, did not significantly differ between HRD groups, suggesting that while gross morphological patterns (shape and bilaterality) are informative, texture-based radiomics features may capture more subtle phenotypic alterations beyond what is discernible by visual assessment(34).

The integration of complementary predictive biomarkers—molecular markers (BRCA, PR) and imaging-derived features (shape, texture)—to construct the proposed combined model yields a biologically plausible framework for preoperative HRD status prediction. The standalone clinical model incorporating BRCA and PR biomarkers achieved an AUC of 0.790–0.805, while the incorporation of radiomic features further elevated the AUC to 0.853–0.889. This marked performance increment indicates that radiomics extracts HRD-associated phenotypic signatures that are not fully captured by molecular markers alone, which may encompass intratumoral heterogeneity, microstructural remodeling, and tumor vascular phenotypes. Collectively, these results substantiate the biological plausibility of our proposed combined model, and underscore the synergistic utility of multi-dimensional data integration for advancing precision oncology practice.

5. Conclusion

In conclusion, this study developed and validated a novel T2WI-based clinical-radiomics combined model for the preoperative prediction of HRD status in patients with HGSOC, offering potential guidance for clinical decision making and merit further evaluations and development for future clinical applications.

6. Limitation and Future Directions

There are limitations in this study. Firstly, this is retrospective research with samples from a single hospital. Secondly, the lack of an external validation cohort limits the generalizability of our findings. Validations with a larger sample size from multi-centers would be conducted in our future work. Finally, the manual segmentation of tumor regions is time-consuming and subject to inter-observer variability, underscoring the need for automated segmentation approaches in future studies.

Abbreviations

T2WI, T2-weighted imaging

HRD, homologous recombination deficiency

HGSOC, high-grade serous ovarian carcinoma

ROC, receiver operating characteristic

AUC, area under the curve

DCA, decision curve analysis

PARPi, poly ADP-ribose polymerase inhibitor

BRCA, breast cancer susceptibility gene

CA125, carbohydrate antigen 125

CEA, carcinoembryonic antigen

HE4, human epididymis protein 4

VOI, volumes of interest

ICC, intraclass correlation coefficient

LASSO, least absolute shrinkage and selection operator

H-L, Hosmer-Lemeshow

SD, standard deviation

PR, progesterone receptor

FIGO, Federation of International of Gynecologists and Obstetricians

ER, estrogen receptor

OR, Odds Ratio

CI, Confidence Interval

PPV, positive predictive value

NPV, negative predictive value

Declarations

Ethics approval and consent to participate

This retrospective study adhered to the Declaration of Helsinki and was approved by the Institutional Review Board (IRB) of the ***, which waived the requirement for informed consent.

Availability of data and materials

The datasets used and/or analysed during the current study are available from the corresponding author on reasonable request.

Conflict of interest

The authors declare that they have no competing interests.

Funding

Not applicable.

References

1. Chen GM, Kannan L, Geistlinger L, et al. Consensus on Molecular Subtypes of High-Grade Serous Ovarian Carcinoma. Clinical cancer research: an official journal of the American Association for Cancer Research. 2018; 24(20):5037–47. DOI:10.1158/1078-0432.Ccr-18-0784.
2. Jayson GC, Kohn EC, Kitchener HC, Ledermann JA. Ovarian cancer. Lancet (London, England). 2014; 384(9951):1376–88. DOI:10.1016/s0140-6736(13)62146-7.
3. Moss HA, Perhanidis JA, Havrilesky LJ, Secord AA. Real-world treatment patterns of maintenance therapy in platinum-sensitive recurrent ovarian cancer. Gynecologic oncology. 2021; 163(1):50–6. DOI:10.1016/j.ygyno.2021.07.026.
4. Ratnaparkhi R, Javellana M, Jewell A, Spoozak L. Evaluation of Homologous Recombination Deficiency in Ovarian Cancer. Current treatment options in oncology. 2024; 25(2):237–60. DOI:10.1007/s11864-024-01176-6.
5. Shah M, Chen TY, Ison G, et al. Overall Survival and the Evolving Benefit-Risk Assessment for Poly (ADP-ribose) Polymerase Inhibitors in Advanced Ovarian Cancer. Journal of clinical oncology: official journal of the American Society of Clinical Oncology. 2025; 43(19):2218–27. DOI:10.1200/jco-24-02834.
6. Cannizzaro MC, Minucci A, Zormpas-Petridis K, et al. Homologous recombination deficiency in Ovarian cancer: The game-changer for first-line maintenance therapy. Critical reviews in oncology/hematology. 2026; 222:105270. DOI:10.1016/j.critrevonc.2026.105270.
7. Nero C, Boldrini L, Lenkowicz J, et al. Deep-Learning to Predict BRCA Mutation and Survival from Digital H&E Slides of Epithelial Ovarian Cancer. Int J Mol Sci. 2022; 23(19). DOI:10.3390/ijms231911326.

8. Watkins JA, Irshad S, Grigoriadis A, Tutt AN. Genomic scars as biomarkers of homologous recombination deficiency and drug response in breast and ovarian cancers. Breast cancer research: BCR. 2014; 16(3):211. DOI:10.1186/bcr3670.
9. Pellegrino B, Mateo J, Serra V, Balmaña J. Controversies in oncology: are genomic tests quantifying homologous recombination repair deficiency (HRD) useful for treatment decision making? ESMO open. 2019; 4(2):e000480. DOI:10.1136/esmoopen-2018-000480.
10. da Cunha Colombo Bonadio RR, Fogace RN, Miranda VC, Diz M. Homologous recombination deficiency in ovarian cancer: a review of its epidemiology and management. Clinics (Sao Paulo, Brazil). 2018; 73(suppl 1):e450s. DOI:10.6061/clinics/2018/e450s.
11. Du J, Zhu L, Duan C, et al. Clinical-genomic characteristics of homologous recombination deficiency (HRD) in breast cancer: application model for practice. European journal of medical research. 2025; 30(1):249. DOI:10.1186/s40001-025-02520-8.
12. Monk BJ, Barretina-Ginesta MP, Pothuri B, et al. Niraparib first-line maintenance therapy in patients with newly diagnosed advanced ovarian cancer: final overall survival results from the PRIMA/ENGOT-OV26/GOG-3012 trial. Annals of oncology: official journal of the European Society for Medical Oncology. 2024; 35(11):981–92. DOI:10.1016/j.annonc.2024.08.2241.
13. Ray-Coquard I, Pautier P, Pignata S, et al. Olaparib plus Bevacizumab as First-Line Maintenance in Ovarian Cancer. N Engl J Med. 2019; 381(25):2416–28. DOI:10.1056/NEJMoa1911361.
14. Jin J, Deng X, Long L, et al. The value of a radiomics model in predicting ovarian malignancy: a retrospective multi-center comparison with O-RADS and radiologists. Insights into imaging. 2025; 16(1):163. DOI:10.1186/s13244-025-02047-w.
15. Wu Y, Zhang Q, Jiang W, Gao Y, Qu B, Wang X. CT-based radiomics predicts HRD score and HRD status in patients with ovarian cancer. Front Oncol. 2024; 14:1477759. DOI:10.3389/fonc.2024.1477759.
16. Boehm KM, Aherne EA, Ellenson L, et al. Multimodal data integration using machine learning improves risk stratification of high-grade serous ovarian cancer. Nature cancer. 2022; 3(6):723–33. DOI:10.1038/s43018-022-00388-9.
17. Qian L, Ren J, Liu A, et al. MR imaging of epithelial ovarian cancer: a combined model to predict histologic subtypes. Eur Radiol. 2020; 30(11):5815–25. DOI:10.1007/s00330-020-06993-5.
18. Thomassin-Naggara I, Aubert E, Rockall A, et al. Adnexal masses: development and preliminary validation of an MR imaging scoring system. Radiology. 2013; 267(2):432–43. DOI:10.1148/radiol.13121161.
19. Avesani G, Tran HE, Cammarata G, et al. CT-Based Radiomics and Deep Learning for BRCA Mutation and Progression-Free Survival Prediction in Ovarian Cancer Using a Multicentric Dataset. Cancers (Basel). 2022; 14(11). DOI:10.3390/cancers14112739.
20. Kojo S, Takada A, Yokota H, et al. CT imaging features as predictors of homologous recombination deficiency and prognosis in high-grade serous ovarian cancer. Abdominal radiology (New York). 2026. DOI:10.1007/s00261-026-05459-4.
21. Zhang S, Yang H, Wang F, et al. Habitat radiomics based on CT for assessing BRCA mutation status in patients with high-grade serous ovarian cancer: a multicenter study. Front Oncol. 2026; 16:1784439.

DOI:10.3389/fonc.2026.1784439.

22. Saida T, Shikama A, Yoshida M, et al. Comparison of MR Imaging of High-grade Serous Carcinomas with and without Homologous Recombination-deficiency. Magnetic resonance in medical sciences: MRMS : an official journal of Japan Society of Magnetic Resonance in Medicine. 2026; 25(1). DOI:10.2463/mrms.mp.2025-0071.
23. Chang YH, Wu KC, Ding DC. Signaling Pathway Dissection After Progesterone Receptor Enhancement in an Immortalized Pre-Cancer Fallopian Tube Epithelial Cell Line. Int J Mol Sci. 2026; 27(9). DOI:10.3390/ijms27094031.
24. Živić K, Boljević I, Nedeljković M, Matović M, Janković R, Tanić M. The Effects of BRCA1 and BRCA2 Promoter Methylation on Clinicopathological Characteristics and Clinical Outcomes in HGSOC. Cells. 2026; 15(3). DOI:10.3390/cells15030277.
25. Konstantinopoulos PA, Spentzos D, Karlan BY, et al. Gene expression profile of BRCAness that correlates with responsiveness to chemotherapy and with outcome in patients with epithelial ovarian cancer. Journal of clinical oncology: official journal of the American Society of Clinical Oncology. 2010; 28(22):3555–61. DOI:10.1200/jco.2009.27.5719.
26. Biglia N, Sgandurra P, Bounous VE, et al. Ovarian cancer in BRCA1 and BRCA2 gene mutation carriers: analysis of prognostic factors and survival. Ecancermedicalscience. 2016; 10:639. DOI:10.3332/ecancer.2016.639.
27. Moschetta M, George A, Kaye SB, Banerjee S. BRCA somatic mutations and epigenetic BRCA modifications in serous ovarian cancer. Annals of oncology: official journal of the European Society for Medical Oncology. 2016; 27(8):1449–55. DOI:10.1093/annonc/mdw142.
28. Hodgson DR, Dougherty BA, Lai Z, et al. Candidate biomarkers of PARP inhibitor sensitivity in ovarian cancer beyond the BRCA genes. British journal of cancer. 2018; 119(11):1401–9. DOI:10.1038/s41416-018-0274-8.
29. Konecny GE, Kristeleit RS. PARP inhibitors for BRCA1/2-mutated and sporadic ovarian cancer: current practice and future directions. British journal of cancer. 2016; 115(10):1157–73. DOI:10.1038/bjc.2016.311.
30. Kawaguchi M, Kato H, Furui T, et al. Prediction of grading of ovarian endometrioid carcinoma using conventional MRI features. Japanese journal of radiology. 2025; 43(5):820–8. DOI:10.1007/s11604-024-01727-9.
31. Takeyama N, Sasaki Y, Ueda Y, et al. Magnetic resonance imaging-based radiomics analysis of the differential diagnosis of ovarian clear cell carcinoma and endometrioid carcinoma: a retrospective study. Japanese journal of radiology. 2024; 42(7):731–43. DOI:10.1007/s11604-024-01545-z.
32. Morioka S, Kawaguchi R, Yamada Y, Iwai K, Yoshimoto C, Kobayashi H. Magnetic resonance imaging findings for discriminating clear cell carcinoma and endometrioid carcinoma of the ovary. Journal of ovarian research. 2019; 12(1):20. DOI:10.1186/s13048-019-0497-1.
33. Qiu J, Ren T, Liu Q, et al. Dissecting the Distinct Tumor Microenvironments of HRD and HRP Ovarian Cancer: Implications for Targeted Therapies to Overcome PARPi Resistance in HRD Tumors and

Refractoriness in HRP Tumors. Advanced science (Weinheim, Baden-Wurttemberg, Germany). 2024; 11(38):e2309755. DOI:10.1002/advs.202309755.

34. Nougaret S, McCague C, Tibermacine H, Vargas HA, Rizzo S, Sala E. Radiomics and radiogenomics in ovarian cancer: a literature review. Abdominal radiology (New York). 2021; 46(6):2308–22. DOI:10.1007/s00261-020-02820-z.

Figures

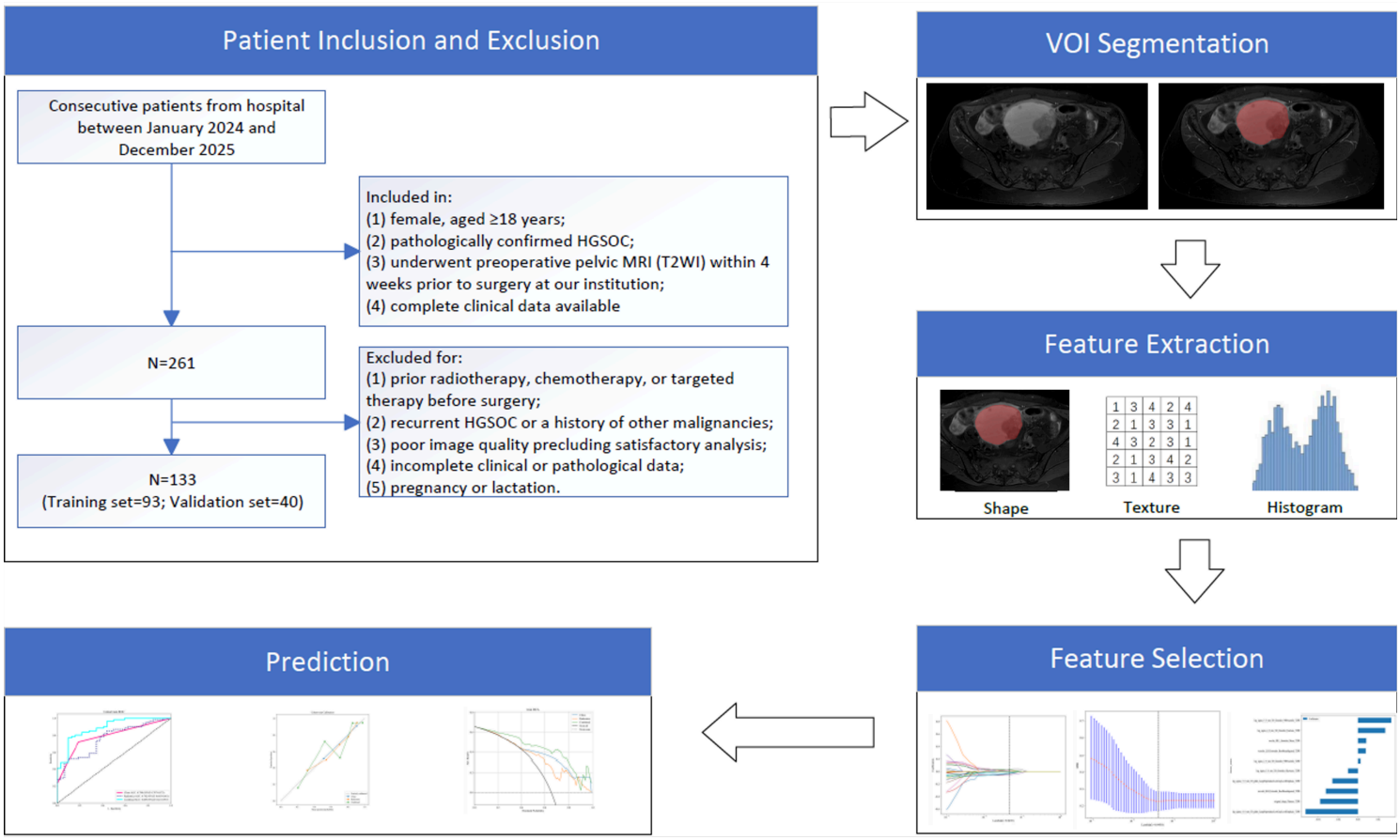


Figure 1

Patient enrollment and workflow of radiomics analysis. Abbreviations: HGSOC, high-grade serous ovarian carcinoma; T2WI, T2 weighted imaging; VOI, volumes of interest.

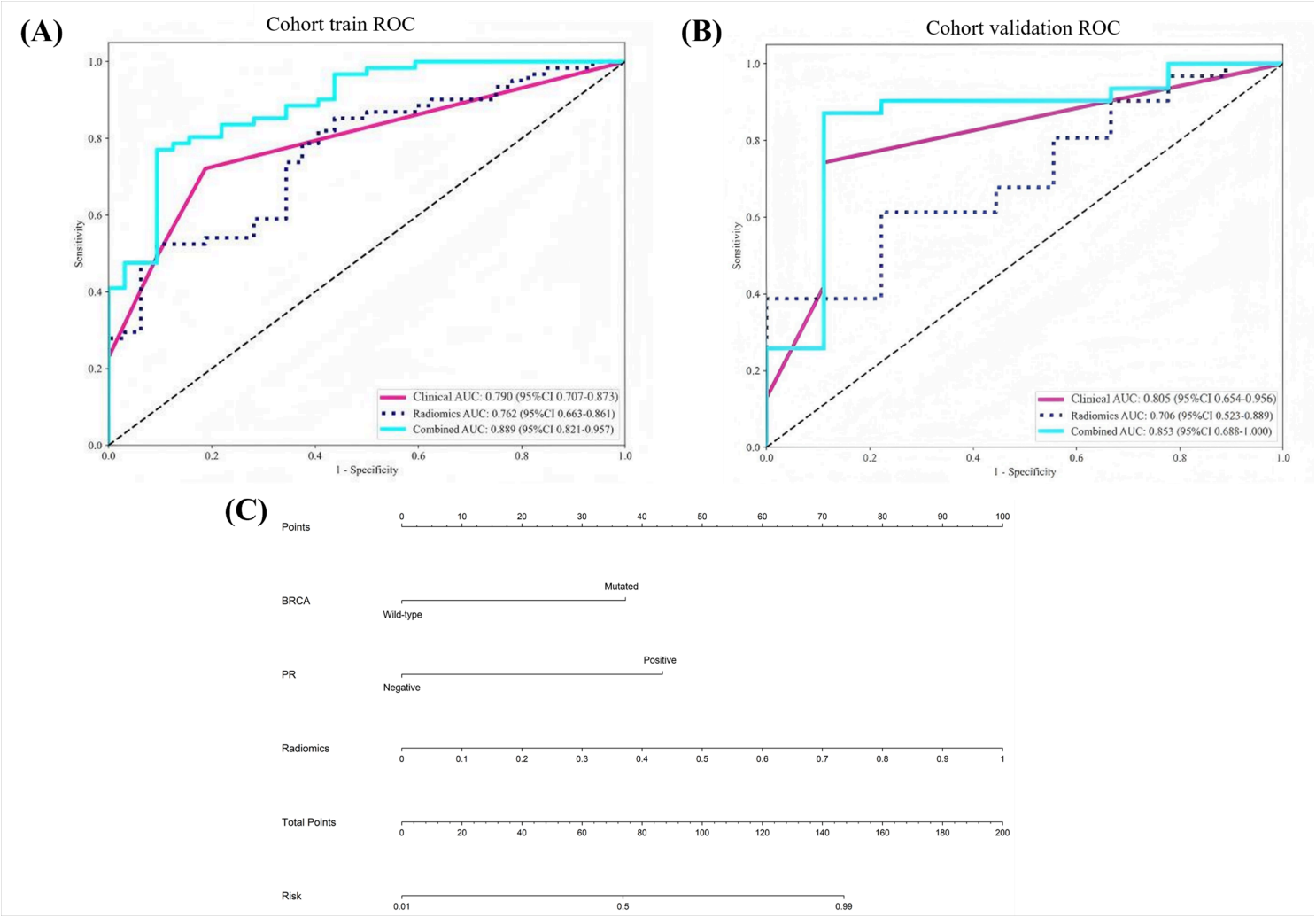


Figure 2

The ROC curves of different models in the training set (A) and validation set (B), and visualization of the nomogram for the combined model (C). The nomogram is constructed by combining BRCA, PR and Radscore. On the point scale axis, each variable was assigned a score. The overall score was calculated by adding each score. We were able to predict the status of HRD using the whole-point scale.
Abbreviations:ROC, receiver operating characteristic; BRCA, breast cancer susceptibility gene; PR, progesterone receptor; HRD, homologous recombination deficiency.

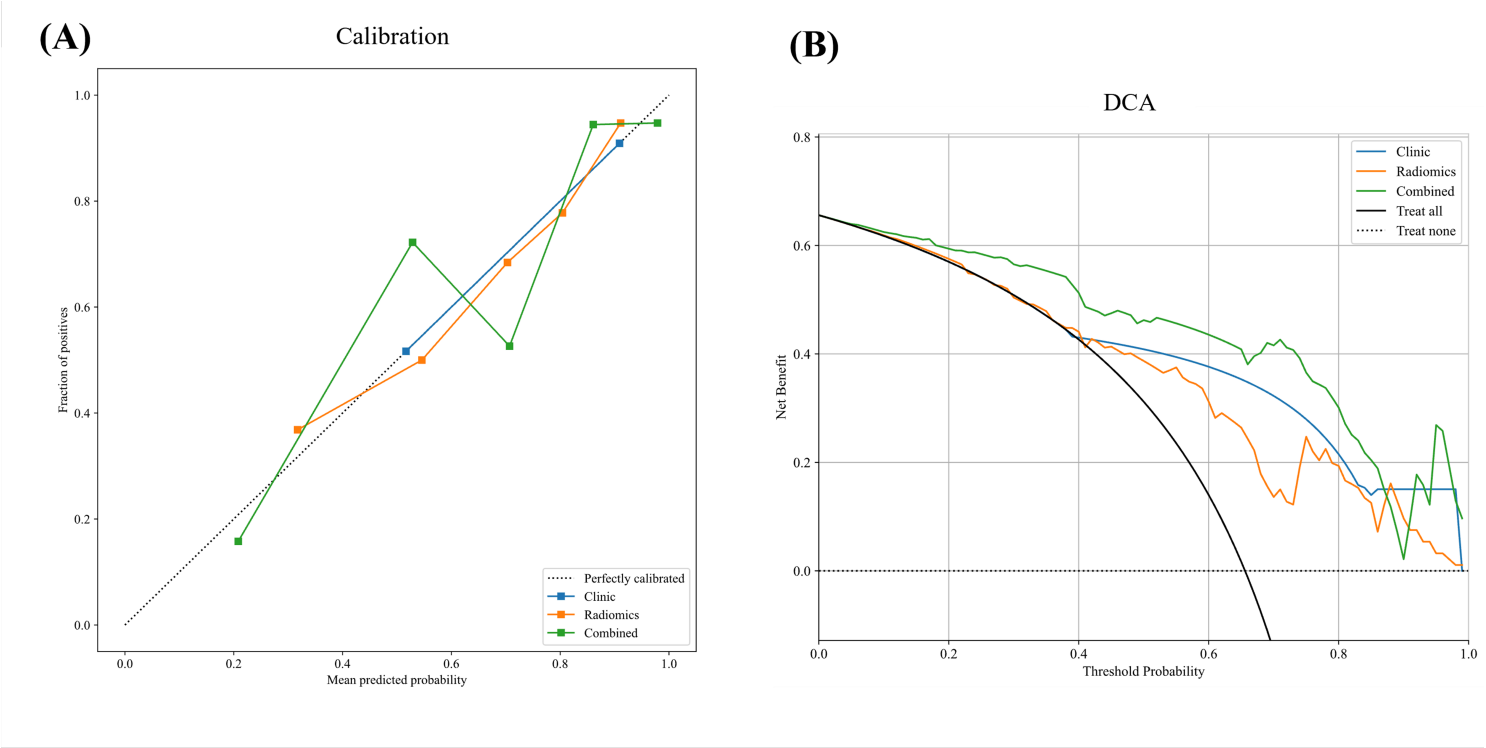


Figure 3

Calibration curves for the combined prediction model (A), and DCA results comparing the combined model, radiomics model, and clinical model (B). Abbreviations: DCA, decision curve analysis.

Supplementary Files

This is a list of supplementary files associated with this preprint. Click to download.

- SupplementaryTable1.docx